Chemical Papers
https://doi.org/10.1007/s11696-023-02827-y

ORIGINAL PAPER

# Pyrene-naphthalimide Schiff base as a fluorescent pigment in water-based security ink

R. S. Bhagya[1] · Kashmitha Muthamma[2] · Dhanya Sunil[2] · Prakasha Shetty[2] · Suresh D. Kulkarni[3]

Received: 18 December 2022 / Accepted: 11 April 2023


## Abstract

Fluorescence-based materials that are affordable and easy to use for commercial anti-counterfeiting applications are in high demand. While exploring new fluorescent pigments, a pyrene-naphthalimide Schiff base, 5-hydroxy-2-((pyren-1-ylmethylene) amino)-1*H*-benzo[*de*]isoquinoline-1,3(2*H*)-dione (NHPY) with yellow fluorescence under UV light was synthesized. An eco-friendly flexographic ink prepared with NHPY as the pigment was coated on a UV dull paper and further printed on security paper as well as packaging papers and boards. When exposed to UV light, the printed samples showed yellow fluorescence. The light fastness, gloss, colorimetric results, and abrasion resistance of the printed samples proved that NHPY is a suitable fluorescent pigment for security printing applications.

**Keywords** Fluorescent pigment · Water-based security ink · Flexographic prints · Anti-counterfeiting

## Introduction

In today's fast-developing technological environment, counterfeit goods and documents that threaten the value of authentic artifacts continue to be a severe problem. Therefore, it is essential to protect them from falsification. In this context, printed non-forgeable security features for use in labels with tamper evidence, security tapes, cheques, postage stamps, bank notes, passports, stock certificates, and identity documents are in high demand (Abdollahi et al. 2020a; Friškovec et al. 2013; Gangwar et al. 2018; Tobias and Everett 2019). It is possible to incorporate non-replicable security components into either the substrate or the printing ink (Abdollahi et al. 2020b; Ataeefard and Nourmohammadian 2015; Hrytsenko et al. 2017; Meng et al. 2014). Fluorescent, thermochromic, hydrochromic, and photochromic colorants have become more prevalent in various security ink applications in the past few decades. However, the quest for colorants with desirable properties continues, and fluorescent pigments, in particular, have been found helpful in a growing number of applications, such as security printing and smart and intelligent packaging (Astuti et al. 2009; Andres et al. 2014; Liu et al. 2019; Abdelhameed et al. 2020). Long- and short-wave UV fluorescent inks find wide applications in anti-counterfeiting. Different classes of fluorophores, including quantum dots, inorganic materials, nanoparticles, complexes of rare-earth elements, and polymer dots, were studied as pigments for security printing (Nuryadin et al. 2017; Nair et al. 2019).

Pyrene possesses a delightful organic structure that could be coupled with various other moieties to create an electron donor-acceptor framework with desirable characteristics. Various derivatives of this polycyclic aromatic hydrocarbon have displayed strong and distinct excimer emission with high fluorescence quantum yield. Though the fluorophore occasionally experiences quenching due to aggregation in solid or concentrated form, pyrene derivatives are used extensively in fluorescent probes, food colorants, OLEDs, biosensors, biomarkers, corrosion inhibitors, printing inks, chemosensors, colorimetric sensors (Kathiravan et al. 2014; Domeño et al. 2017; Shen et al. 2019; Srinivasan et al. 2021; Wang 2021), electroluminescent devices, paints,

✉ Prakasha Shetty
prakash.shetty@manipal.edu

[1] Department of Media Technology, Manipal Institute of Technology, Manipal Academy of Higher Education, Manipal, Karnataka 576104, India

[2] Department of Chemistry, Manipal Institute of Technology, Manipal Academy of Higher Education, Manipal, Karnataka 576104, India

[3] Department of Atomic and Molecular Physics, Centre for Applied Nanosciences, Manipal Academy of Higher Education, Manipal, Karnataka 576104, India

Published online: 17 April 2023

**Scheme 1** Synthetic route for NHPY

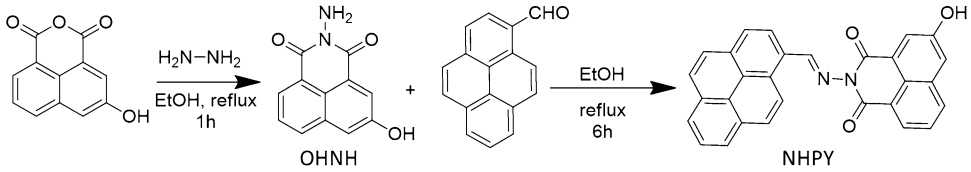


optoelectronics, (Gowri et al. 2020; Jeyasingh et al. 2021; Kr et al. 2021; Uzun 2021; Yao et al. 2021), and anti-counterfeiting (Maeda et al. 2001; Homa et al. 2017; Mohamed et al. 2020; Boonnab et al. 2021). Although various colorants are available, very few inks, such as bio-ink and tattoo inks, have been developed utilizing pyrene, primarily for inkjet and 3D printing. The majority of the pyrene-based inks used for anti-counterfeiting applications are probed as writing or painting ink (Sonawane and Asha 2016; Wakchaure et al. 2019; Lone et al. 2019; Qiu et al. 2020; Shi et al. 2021), and rarely they are screen or inkjet printed (Chen et al. 2019; Wang et al. 2021). There are only two detailed reports on pyrene derivatives used in water-based flexographic inks (Bhagya et al. 2021; Muthamma et al. 2021). Naphthalimide is yet another organic fluorophore reported as a pigment in writing and inkjet printing inks. However, most of them are just solutions of the pigment in a suitable solvent (Tan et al. 2018; Yang et al. 2018; Dwivedi et al. 2018; Ni et al. 2019; Pati et al. 2020; Rani and Sengupta 2021; Chen et al. 2022; Kumar et al. 2022) and are not standard ink formulations, except for a report on water-based flexographic ink (Muthamma et al. 2022).

Therefore, in this study a new pyrene-naphthalimide hybrid molecule: NHPY is prepared via a two-step synthetic approach as a fluorescent pigment. The structural, photophysical, and thermal features of NHPY are explored for its possible use as a pigment in a water-based security ink formulation. Further, the ink prepared was printed using flexography on different substrates such as security papers, packaging papers, and boards. The prints obtained using NHPY ink offered good light fastness, gloss, photoluminescence, colorimetric properties, and abrasion resistance. The eco-friendly flexographic inks find their role in Pantone colors, security, and other anti-counterfeiting applications.

## Experimental

### Synthesis and characterization

The solvents and chemicals utilized in this investigation were procured from Sigma, Spectrochem, and Finar Chemicals.

### 2-amino-5-hydroxy-1*H*-benzo[*de*] isoquinoline-1,3(2*H*)-dione (OHNH)

Hydrazine hydrate (1.86 mmol) was added to 3-hydroxy-1,8-naphthalic anhydride (0.37 mmol) dissolved in 30 mL ethanol. The reaction mixture was refluxed for 1 h, quenched with distilled water, and left aside overnight. The precipitate formed was filtered and washed with distilled water to obtain OHNH.

### 5-hydroxy-2-((pyren-1-ylmethylene) amino)-1H-benzo[de]isoquinoline-1,3(2H)-dione (NHPY)

An equimolar mixture of OHNH and 1-pyrene carbaldehyde in 20 mL of ethanol was refluxed for 6 h at 80 °C. The precipitate formed was filtered and washed with hot ethanol (15 mL) to obtain yellow-colored NHPY. The synthetic pathway is depicted in Scheme 1.

The melting points of OHNH and NHPY were determined by the open capillary method. The chemical structures of both molecules were validated by recording the IR (Shimadzu IR Spirit spectrophotometer), NMR (400 MHz Bruker spectrophotometer), and mass spectra (Agilent 6430 Triple Quad with electrospray ionization). The chemical structures of OHNH and the NHPY were confirmed using spectral techniques and are presented below. The IR, $^{1}$H, and $^{13}$C NMR spectra confirmed the molecular structures. The $D_2O$ exchange spectra helped to recognize the presence of labile protons. Mass spectra established the molecular weight of the naphthalimide derivatives.

### 2-amino-5-hydroxy-1*H*-benzo[*de*] isoquinoline-1,3(2*H*)-dione (OHNH)

Yellow powder (75.67%); m.p: > 250 °C; ATR-IR ($cm^{-1}$) 3613, 3254 (O–H & N–H *str.*), 3037 (Ar. C–H *str.*), 1694 (C=O *str.*) (Supplementary Figure, Fig. S1); $^{1}$H NMR (DMSO, 400 MHz): δ 10.57 (s, OH, 1H), 8.289–8.270 (d, 1H, 7.6 Hz), 8.263–8.241 (d, 1H, 8.8 Hz), 8.038 (s, 1H), 7.775–7.737 (t, 1H, 7.6 Hz), 7.669 (s, 1H), 5.77 (s, $NH_2$, 2H) (Fig. S2); $^{1}$H NMR ($D_2O$ exchange, 400 MHz) (Fig. S3); $^{13}$C

NMR (DMSO, 100 MHz): 161.12, 160.72, 156.62, 133.75, 133.25, 128.06, 127.84, 123.53, 122.29, 121.98, 121.22, 116.33 (Fig. S4); MS $C_{12}H_8N_2O_3$ (ESI, *m/z*): 228.20 (calculated), 227.00 (experimental) (Fig. S5).

### 5-hydroxy-2-((pyren-1-ylmethylene) amino)-1*H*-benzo[*de*]isoquinoline-1,3(2*H*)-dione NHPY

Yellow powder (70.60%); m.p: > 250 °C; ATR-IR ($cm^{-1}$) 3288 (O–H), 1662 (C=O) (Fig. S6); $^1$H NMR (DMSO, 400 MHz): δ 10.65 (s, OH, 1H), 9.814 (s, CH=N, 1H), 9.026–9.003 (d, 1H, 9.2 Hz), 8.795–8.775 (d, 1H, 8 Hz), 8.498–8.324 (m, 8H), 8.215–8.140 (m, 2H), 7.851–7.813 (t, 1H, 7.6 Hz), 7.757 (s, 1H) (Fig. S7); $^1$H NMR ($D_2O$ exchange, 400 MHz) (Fig. S8); $^{13}$C NMR (DMSO, 100 MHz) (Fig. S9): δ 171.89, 161.14, 160.76, 156.69, 134.18, 133.93, 133.41, 131.16, 130.71, 130.47, 130.11, 129.99, 128.42, 127.96, 127.85, 127.33, 127.20, 127.07, 126.92, 125.64, 125.33, 124.42, 124.26, 123.95, 123.36, 122.70, 122.60, 122.10, 116.57; MS $C_{29}H_{16}N_2O_3$ (ESI, *m/z*): 440.45 (calculated), 439.05, 440.10 (experimental) (Fig. S10); Elemental analysis: % calculated C-79.08, H-3.66, N-6.36; % found C-77.05, H-3.95, N-6.27.

### Intrinsic features of NHPY

The absorption (1800 Shimadzu UV–visible spectrophotometer) and emission spectra JASCO spectrofluorometer FP 8300) of NHPY were recorded. Photoluminescence measurements were conducted at 370 nm excitation wavelength. All theoretical simulations were performed in a vacuum using a 6-31G + + basis set and the B3LYP functions of Schrödinger's materials science suite. Hitachi simultaneous thermogravimetric analyzer (STA7000 series) was used to analyze the thermal stability of NHPY.

### Ink formulation and flexo print features

Kamicryl 2077 and 2074 (Kamsons Chemicals) were used as acrylic emulsions. The OT 75 (Spak Organochem) and Joncryl 35 (BASF) were used as wetting and dispersion agents, correspondingly. Tego foamex 0843 and carbitol (Diethylene glycol monoethyl ether) were supplied by Evonik and DOW chemicals, respectively. The NHPY pigment was milled using a Lloyds pigment miller (92 N at 40 Kgf). The fineness of the grind of NHPY in ink was determined using the Zehntner grind meter.

The thickness (Mitutoyo thickness gauge) and grammage (Digital GSM tester) of the substrates: UV dull paper (Manipal Technologies), Kraft papers (Mysore Kraft), and Chrome art (Sun paper), Duplex board (West coast) and Ivory boards (Bilt) were measured. The substrate surfaces were coated with the ink using a K bar coater (zero number), and 10.5 cm × 29.7 cm patches were printed with RK Flexiproof 100 at a speed of 50 m/min using 9.5 BCM anilox roll, chambered inking system, and a photopolymer plate. The XRD (X-Ray Diffraction) plots of the dried ink layer were recorded with Rigaku Miniflex 600 at 2$\theta$ range of 5 to 80° and a scan rate of 4° per minute using CuKα radiation at a wavelength of 1.54 Å. The colorimetric values (color density, *L*, *a*, *b*, and Δ*E*) were evaluated using an Xrite I1 Pro spectrophotometer. The light fastness (Hari Impex LAB UV 83,002) and gloss (Truesize gloss meter) of the ink film were assessed. Sutherland ink abrasion tester was used to check the abrasion resistance of printed ink film on substrates at 50 rubs using 2 lb weight. The surface morphological properties of the printed sample were examined using a secondary electron mode detector analytical scanning electron microscope (Carl Zeiss EVO 18 SEM).

## Results and discussion

The absorption spectrum of $1 \times 10^{-5}$ M solution of OHNH and NHPY in DMSO was recorded, and the absorbance maxima were observed at around 338 and 392 nm, and 340 and 398 nm, for $\pi - \pi^*$ and $n - \pi^*$ transitions, respectively (Fig. S11). The solid-state photoluminescence studies revealed maximum excitation wavelength ($\lambda_{ex}$) for both the molecules at 370 nm (Fig. S12) and maximum fluorescence emission ($\lambda_{em}$) at 597 nm for OHNH and 549 nm for NHPY (Fig. S13). As NHPY was found to show intense emission compared to OHNH, further studies were performed using the pyrene-naphthalimide derivative.

The flexographic ink must withstand the heat applied to the substrate, which can extend up to 200 °C during various finishing operations such as heat sealing and lamination (for plastic substrates), ironing (for textile substrates), etc. Therefore, the thermogravimetric analysis (TGA) of NHPY was performed. The TGA plots (Fig. 1a) did not show any weight loss up to 300 °C revealing the thermal stability, which is adequate for a pigment in printing ink.

Water-based flexographic ink with improved eco-friendliness was formulated using NHPY as the fluorescent pigment to replace solvent-based inks and thereby reduce the volume of VOC emission. The ink was prepared in two stages: In step 1, the NHPY pigment, Kamicryl 2074 Acrylic emulsion, wetting and dispersing agent (OT 75), and thinner (Carbitol) were weighed and milled in the Lloyds pigment miller to produce the ink concentrate. In step 2, the pigment concentrate and remaining components as mentioned in Table 1 were mixed in a magnetic stirrer to obtain the final ink for flexographic printing (Elsawy et al. 2021). The % composition of NHPY ink is presented in Table 1.

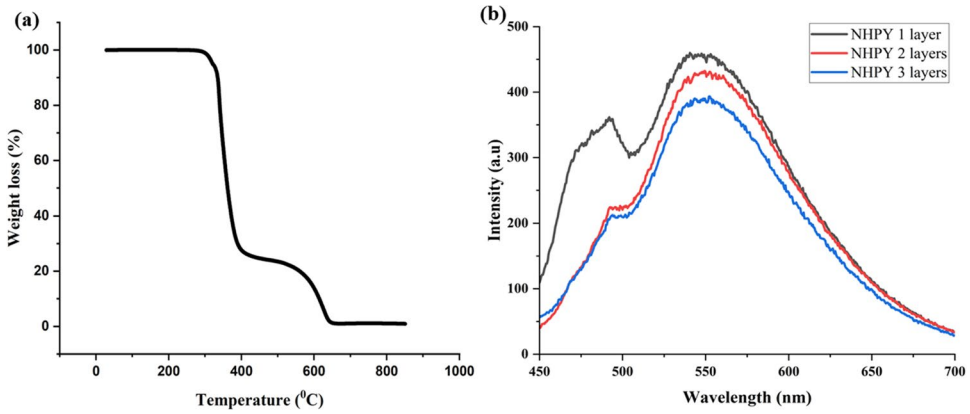


**Fig. 1** **a** Thermogravimetric plots of NHPY and **b** emission spectra of different coating layers ($\lambda_{ex} = 370$ nm)

**Table 1** Formulation of pigment concentrate and final ink

| Components | Mass (grams) | % composition |
|---|---|---|
| Ink concentrate | | |
| NHPY | 0.62 | 12.09 |
| Kamicryl 2074 (Acrylic emulsion 1) | 3.78 | 73.68 |
| OT 75 (Wetting and Dispersing agent, WDA) | 0.05 | 0.97 |
| Carbitol | 0.68 | 13.26 |
| Ink formulation | | |
| Pigment concentrate | 5.13 | 56.19 |
| Kamicryl 2074 (Acrylic emulsion 1) | 1.5 | 16.43 |
| Kamicryl 2077 (Acrylic emulsion 2) | 1.5 | 16.43 |
| Joncryl 35 (Wax) | 0.17 | 1.85 |
| Tego foamex 0843 (Defoamer) | 0.03 | 0.33 |
| Water | 0.7 | 7.67 |
| Aqueous ammonia | 0.1 | 1.1 |

The resin constituents of acrylic emulsions can influence the physical and chemical properties of ink as well as the ink film. These resins wet the pigment properly and bind it to the substrate. Resins enhance the drying properties, rub resistance, and gloss of the printed ink. The silicone-based surfactant OT 75 was used as the wetting and dispersing agent to improve pigment wetting and decrease surface tension. The rub resistance and surface slip of the printed ink film are enhanced with Joncryl 35 wax. Carbitol is used as a thinner to control the ink viscosity. Tego foamex 0843 prevents foaming and subsequent printing defects. Emulsions and acidic acrylic resins were stabilized using the charge repulsion technique in the water-based system using aqueous ammonia. De-ionized water acted as the solvent.

The NHPY ink was prepared as per the standard formulation used in the industry for water-based flexographic printing. The pH of the prepared ink was found to be 8.7 (the standard range for water-based ink is 8.5–9.5). Further, the viscosity of the NHPY ink was measured using Ford cup B4 and was found to be 25 s (the standard range for water-based ink is 25–30 s). An even pigment dispersion is required for the ink's performance on the printing machine. Particle agglomerates can have a variety of effects on both the printing procedure and the print quality. Consequently, the particle size of NHPY was determined using a grind gauge and was found to be $< 5$ µm. To find the nature of the ink, XRD plots of the dried ink film (Fig. S14) were analyzed, which showed that the ink particles were crystalline. The external quantum efficiency of the NHPY ink was 1.56%.

The drawdown method was used to assess the ink's color mixing, drying characteristics, and performance on the substrate. The coating using NHPY ink on a UV dull paper appeared yellow under daylight and showed greenish-yellow fluorescence on exposure under 365 nm UV light (Fig. S15). The influence of fluorescence intensity on coating thickness was studied by coating different layers of NHPY ink and evaluating its photoluminescence. The fluorescence spectra shown in Fig. 1b for the multiple coats using NHPY ink depicted the highest fluorescence for three layers. However, insignificant changes in the emission intensity observed in the coats suggest that ink film thickness does not impact the fluorescence emission when viewed with the naked eye under UV illumination.

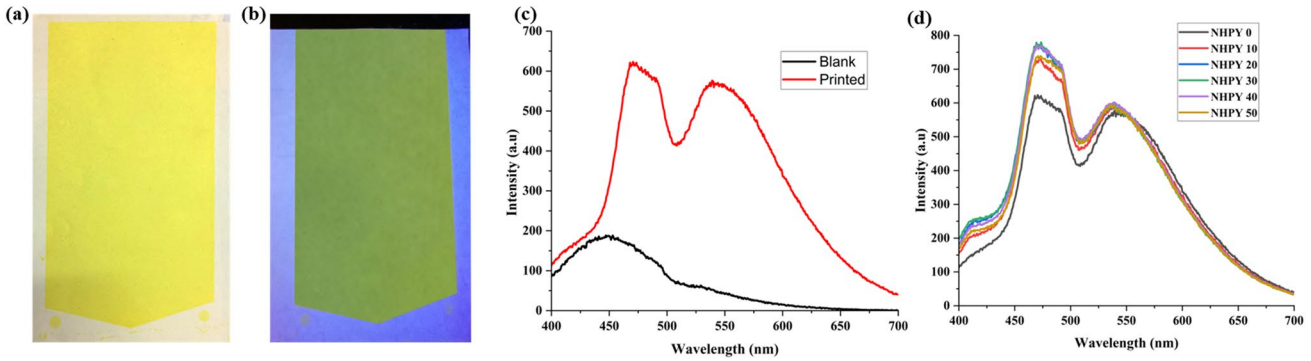


**Fig. 2** Photographs of UV dull paper printed with NHPY ink observed **a** in daylight, **b** under UV light. **c** The emission spectra of blank and printed UV dull paper and **d** print proof subjected to light-fastness test ($\lambda_{ex} = 370$ nm)

**Table 2** Colorimetric values of printed NHPY ink layer

| Substrate | Colorimetric values | | | |
|---|---|---|---|---|
| | Density | *L* | *a* | *b* |
| UV dull paper | 0.36 | 91.66 | − 16.51 | 41.19 |
| Chrome art paper | 0.38 | 89.51 | − 17.31 | 40.72 |
| Kraft paper | 1.07 | 53.94 | − 1.35 | 37.1 |
| Duplex board | 0.43 | 87.1 | − 16.82 | 42.88 |
| Ivory board | 0.44 | 86.91 | − 19.21 | 44.21 |

Five different substrates were printed on Ivory and Duplex board, Chrome art and Kraft papers, and UV dull paper using flexography. All flexographic printing substrates must comply with ISO 12647-6 and possess color values $L \geq 90$, $a \leq 3$, and $b \leq 5$ (Tipsotnaiyana et al. 2015). All the substrates comply with ISO 12647-6 requirements, excluding the Kraft paper, (Elsawy et al. 2021) due to its brown color. Supplementary Table 1 (Table ST1) lists the characteristics of these substrates. The developed NHPY ink was printed on all five substrates using the flexographic technique. The photographs of the print on UV dull security paper in daylight (Fig. 2a) and under UV light (Fig. 2b) depict visual appearance. A security paper lacking optical brighteners will not interfere with fluorescence emission or other security features of the ink. Thus, the blue emission on the blank paper is minimal and negligible compared to the printed substrate emission. (Fig. 2c).

All the substrates used for printing in the present study had low gloss, except the duplex board and chrome art paper. NHPY print on UV dull paper had a gloss value of 5.2 GU (Gloss Unit) at 60° measurements, which is less than 10 as per the standard for low gloss paper. High gloss papers have a gloss rating of over 70 GU, whereas medium gloss papers are those with a gloss rating range between 10 and 70 GU(Sönmez and Arslan 2021). Table 2 illustrates the color density, L, a, and b values of the NHPY ink layer on different printed substrates. Since all the b values were positive, yellow is shown by print proof. Except for Kraft paper, all papers had values around 10, indicating an ashen shade of yellow. Further, the *L* values exceeded 90, which specified the nearest match to white. As a result, the ink layer is intensely yellow.

To check the light fastness of the ink layer, the colorimetric values for the substrates printed with NHPY ink were measured with a UV curing apparatus at 10, 20, 30, 40, and 50 passes as per industry standards. The measured colorimetric values are tabulated in Table 3. Compared to the strength of typical UV radiation (around 6.5 mW/cm$^2$), the lamps used in the Hari Impex lab UV dryer have an intensity of 15–25 W/cm$^2$. The study was conducted for 50 cycles, a reasonably long exposure time. The emission spectra of the UV-exposed and unexposed samples were obtained as depicted in Fig. 2d. The fluorescence of the UV-exposed samples did not show any significant difference in emission intensity, which revealed that the pigment had good

**Table 3** Light fastness of NHPY ink printed on UV dull paper

| Colorimetric values | Paper reference | No. of passes | | | | | |
|---|---|---|---|---|---|---|---|
| | | 0 | 10 | 20 | 30 | 40 | 50 |
| Density | 0.61 | 0.61 | 0.60 | 0.60 | 0.59 | 0.60 | 0.60 |
| L | 93.4 | 93.5 | 93.4 | 93.3 | 93.3 | 93.0 | 92.9 |
| a | − 9.7 | − 9.5 | − 8.9 | − 8.6 | − 8.4 | − 8.3 | − 8.3 |
| b | 38.6 | 39.1 | 38.9 | 39.1 | 38.6 | 38.6 | 38.4 |
| ΔE | 17.5 | 17.3 | 17.2 | 17.2 | 17.0 | 17.0 | 17.0 |

**Table 4** Colorimetric values of printed samples before and after the abrasion test

| Substrate | Colorimetric values | | | | | | | | | | $\Delta E$ difference before and after the test |
|---|---|---|---|---|---|---|---|---|---|---|---|
| | Before test | After test | Before test | | | | After test | | | | |
| | Density | | $L$ | $a$ | $b$ | $\Delta E$ | $L$ | $a$ | $b$ | $\Delta E$ | |
| UV dull paper | 0.61 | 0.11 | 93.4 | −9.7 | 38.6 | 17.5 | 90.5 | −9.3 | 37.9 | 19 | 1.5 |
| Chrome art | 0.09 | 0.09 | 91.8 | −9.1 | 38.9 | 23.1 | 91.6 | −9.6 | 38.1 | 21.9 | 1.2 |
| Kraft | 1.05 | 1.07 | 61.2 | 2.5 | 32.0 | 6.7 | 59.4 | 3.9 | 31.0 | 6.4 | 0.3 |
| Duplex board | 0.74 | 0.74 | 89.9 | −9.3 | 41.2 | 18.4 | 90.2 | −9.3 | 41.8 | 18.3 | 0.1 |
| Ivory board | 0.12 | 0.13 | 89.5 | −10.4 | 38.3 | 31.0 | 89.1 | −10.4 | 38.5 | 31.6 | 0.6 |

photostability. Additionally, the prints displayed good light stability even after being exposed to ambient conditions for 6 months.

The abrasion test illustrates the damage that might result if the paper rubs against a printed image while being transported. The colorimetric values measured after the rub test on the printed substrates are listed in Table 4. The $\Delta E$ values were calculated using the equation: (Ozcan 2019)

$$\Delta E = \sqrt{(\Delta L)^2 + (\Delta a)^2 + (\Delta b)^2}$$

where $\Delta L = L_2 - L_1$, $\Delta a = a_2 - a_1$ and $\Delta b = b_2 - b_1$. $L_1$, $a_1$, $b_1$, and $L_2$, $a_2$, $b_2$ are the values before and after the abrasion test. Normally, a $\Delta E$ value of 0–2 is typically impossible for the human eye to detect, while a color specialist can recognize a value of 2–3, and if $\Delta E > 3$ it can be noticed easily by everyone. For most papers printed using NHPY ink, $\Delta E < 3$, as revealed in Table 4, indicating good ink film abrasion resistance (Sönmez and Arslan 2021).

## Conclusion

Very few studies have been reported on naphthalimide-based inks and they are mere writing and inkjet printing inks. Moreover, all these reported inks were just solutions of pigments using a suitable solvent. A new pyrene-naphthalimide pigment NHPY with intense yellow fluorescence was synthesized. The structural, photophysical, and thermal properties of NHPY were investigated. A water-based flexographic printing was prepared using this pigment, bar-coated, and printed on several substrates. The ink demonstrated good adhesion, light fastness, gloss, fluorescence, and abrasion resistance on paper and paperboard substrates. The NHPY ink has promising security printing, packaging, and anti-counterfeiting applications.

**Supplementary Information** The online version contains supplementary material available at https://doi.org/10.1007/s11696-023-02827-y.

**Acknowledgements** We thank Mr. P.J Anand and Dr. Shivananda Wagle from Manipal Technologies limited for providing the materials and laboratory facilities for ink formulation and printing.

**Author contributions** PS: supervision and manuscript reviewing; DS: conceptualization and methodology; BRS: experiment conduction, data collection, and manuscript preparation; KM: chemical characterization; SDK: photoluminescence studies.

**Funding** Open access funding provided by Manipal Academy of Higher Education, Manipal.

## Declarations

**Conflict of interest** The authors declare no conflict of interest.



## References

Abdelhameed MM, Attia YA, Abdelrahman MS, Khattab TA (2020) Photochromic and fluorescent ink using photoluminescent strontium aluminate pigment and screen printing towards anticounterfeiting documents. Luminescence 36(4):865–874. https://doi.org/10.1002/bio.3987

Abdollahi A, Roghani-Mamaqani H, Razavi B, Salami-Kalajahi M (2020a) Photoluminescent and chromic nanomaterials for anticounterfeiting technologies: recent advances and future challenges. ACS Nano 14:14417–14492. https://doi.org/10.1021/acsnano.0c07289

Abdollahi A, Roghani-Mamaqani H, Salami-Kalajahi M, Razavi B, Sahandi-Zangabad K (2020b) Encryption and optical authentication of confidential cellulosic papers by ecofriendly multi-color photoluminescent inks. Carbohydr Polym 245:116507. https://doi.org/10.1016/j.carbpol.2020.116507

Abdullah M, Astuti K (2009) Synthesis of luminescent ink from europium-doped $Y_2O_3$ dispersed in polyvinyl alcohol solution. Adv Optoelectron 9:918351. https://doi.org/10.1155/2009/918351

Andres J, Hersch RD, Moser JE, Chauvin AS (2014) A new anti-counterfeiting feature relying on invisible luminescent full color images printed with lanthanide-based inks. Adv Funct Mater 24:5029–5036. https://doi.org/10.1002/adfm.201400298

Ataeefard M, Nourmohammadian F (2015) Producing fluorescent digital printing ink: Investigating the effect of type and amount of coumarin derivative dyes on the quality of ink. J Lumin 167:254–260. https://doi.org/10.1016/j.jlumin.2015.06.042

Bhagya RS, Sunil D, Shetty P, Kagatikar S, Wagle S, Melroy Lewis P, Kulkarni SD, Kekuda D (2021) Water-based flexographic ink using chalcones exhibiting aggregation-induced enhanced emission for anti-counterfeit applications. J Mol Liq 344:117974. https://doi.org/10.1016/j.molliq.2021.117974

Boonnab S, Chaiwai C, Nalaoh P, Manyum T (2021) Synthesis, characterization, and physical properties of pyrene-naphthalimide derivatives as emissive materials for electroluminescent devices. European J Org Chem 17:2402–2410. https://doi.org/10.1002/ejoc.202100134

Chen L, Hu B, Zhang J, Zhang J, Huang S, Ren P, Zou Y, Ding F, Liu X, Li H (2019) A facile synthesis of 1,3,6,8-pyrenesulfonic acid tetrasodium salt as a hydrosoluble fluorescent ink for anti-counterfeiting applications. RSC Adv 9:476–481. https://doi.org/10.1039/C8RA09106D

Chen C, Zhang T, Zhou X, Lin H, Cui J, Liu X, Li H (2022) Fluorescent self-healing waterborne polyurethane based on naphthalimide derivatives and its application in anti-counterfeiting. Prog Org Coat 167:106826. https://doi.org/10.1016/j.porgcoat.2022.106826

Domeño C, Aznar M, Nerín C, Isella F, Fedeli M, Bosetti O (2017) Safety by design of printed multilayer materials intended for food packaging. Food Addit Contam Part A Chem Anal Control Expo Risk Assess 34:1239–1250. https://doi.org/10.1080/19440049.2017.1322221

Dwivedi SK, Gupta RC, Srivastava P, Singh P, Koch B, Maiti B, Misra A (2018) dual fluorophore containing efficient photoinduced electron transfer based molecular probe for selective detection of Cr3+ and PO43- Ions through fluorescence "Turn-On-Off" response in partial aqueous and biological medium: live cell imaging and logic application. Anal Chem 90(18):10974–10981. https://doi.org/10.1021/acs.analchem.8b02570

Elsawy MM, Faheim AA, Salem SS, Owda ME, Abd El-Wahab ZH, Abd El-Wahab H (2021) Cu (II), Zn (II), and Ce (III) metal complexes as antimicrobial pigments for surface coating and flexographic ink. Appl Organomet Chem 35(5):e6196. https://doi.org/10.1002/aoc.6196

Friškovec M, Kulčar R, Gunde MK (2013) Light fastness and high-temperature stability of thermochromic printing inks. Color Technol 129:214–222. https://doi.org/10.1111/cote.12020

Gangwar AK, Nagpal K, Gupta BK (2018) Triluminescent functional composite pigment for non-replicable security codes to combat counterfeiting. ChemistrySelect 3:9627–9633. https://doi.org/10.1002/slct.201801938

Gowri A, Khamrang T, Velusamy M, Kathiresan M (2020) Pyrene based chemosensor for carbon dioxide gas meticulous investigations and digital image based RGB analysis. Sens Actuators Rep 2:100007. https://doi.org/10.1016/j.snr.2020.100007

Homa P, Tryba B, Gęsikiewicz-Puchalska A (2017) Impact of paint matrix composition and thickness of paint layer on the activity of photocatalytic paints. Pol J Chem Technol 19:113–119. https://doi.org/10.1515/pjct-2017-0016

Hrytsenko O, Shvalagin V, Grodziuk G, Granchak V (2017) Influence of parameters of screen printing on photoluminescence properties of nanophotonic labels for smart packaging. J Nanotechnol 2017:7125682. https://doi.org/10.1155/2017/7125682

Jeyasingh V, Murugesan K, Lakshminarayanan S, Selvapalam N (2021) Pyrene-hydrazone-π ··· Hole coupled turn-on fluorescent and naked-eye colorimetric sensor for cyanide: role of homogeneous π-hole dispersion in anion selectivity. J Fluorescence 31:1303–1309. https://doi.org/10.1007/s10895-021-02765-6

Kathiravan A, Sundaravel K, Jaccob M, Dhinagaran G, Rameshkumar A, Ananth DA, Sivasudha T (2014) Pyrene Schiff base: photophysics, aggregation induced emission, and antimicrobial properties. J Phys Chem B 118(47):13573–13581. https://doi.org/10.1021/jp509697n

Kr S, Murmu M, Chandra N, Banerjee P (2021) Synthesis, characterization and theoretical exploration of pyrene based Schiff base molecules as corrosion inhibitor. J Mol Struct 1245:131098. https://doi.org/10.1016/j.molstruc.2021.131098

Kumar S, Sharma N, Kaur S, Singh P (2022) Pseudo-crown ether III: Naphthalimide-Pd(II) based fluorogenic ensemble for solution, vapour and intracellular detection of amine and anti-counterfeiting applications. J Photochem Photobiol A Chem 430:113974. https://doi.org/10.1016/j.jphotochem.2022.113974

Liu F, Nattestad A, Naficy S, Han R, Casillas G (2019) Fluorescent carbon- and oxygen-doped hexagonal boron nitride powders as printing ink for anticounterfeit applications. Adv Optical Mater 7(24):1901380. https://doi.org/10.1002/adom.201901380

Lone MS, Afzal S, Chat OA, Bhat PA, Dutta R, Zhang Y, Kundu N, Dar AA (2019) Broad spectrum tunable photoluminescent material based on cascade fluorescence resonance energy transfer between three fluorophores encapsulated within the self-assembled surfactant systems. J Phys Chem B 123:9699–9711. https://doi.org/10.1021/acs.jpcb.9b07139

Maeda H, Inoue Y, Ishida H, Mizuno K (2001) UV absorption and fluorescence properties of pyrene derivatives having trimethylsilyl, trimethylgermyl, and trimethylstannyl groups. Chem Lett 30(12):1224–1225. https://doi.org/10.1246/cl.2001.1224

Meng X, Kim S, Puligundla P, Ko S (2014) Carbon dioxide and oxygen gas sensors-possible application for monitoring quality, freshness, and safety of agricultural and food products with emphasis on importance of analytical signals and their transformation. J Korean Soc Appl Biol Chem 57:723–733. https://doi.org/10.1007/s13765-014-4180-3

Mohamed M, Gamal M, Kuo S (2020) Pyrene-functionalized tetraphenylethylene polybenzoxazine for dispersing single-walled carbon nanotubes and energy storage. Compos Sci Technol 199:108360. https://doi.org/10.1016/j.compscitech.2020.108360

Muthamma K, Sunil D, Shetty P, Kulkarni SD, Anand PJ (2021) Eco-friendly flexographic ink from fluorene-based Schiff base pigment for anti-counterfeiting and printed electronics applications. Prog Org Coat 161:106463. https://doi.org/10.1016/j.porgcoat.2021.106463

Muthamma K, Sunil D, Kulkarni SD, Anand PJ, Ali T, Kekuda D (2022) Water-based combifuge ink with unique tamper-evident features for anti-counterfeiting applications. J Mol Liq 161:119695. https://doi.org/10.1016/j.molliq.20221.119695

Nair KS, Abhilash P, Surendran KP (2019) Silica-based organic-inorganic hybrid fluorescent ink for security applications. ACS Omega 4(2):2577–2583. https://doi.org/10.1021/acsomega.8b03313

Ni Y, Sun Z, Wang Y, Nour HF, Sue ACH, Finney NS, Baldridge KK, Olson MA (2019) Versatile hydrochromic fluorescent materials based on a 1,8-naphthalimide integrated fluorophore-receptor system. J Mater Chem C Mater 7:7399–7410. https://doi.org/10.1039/c9tc01304k

Nuryadin BW, Nurjanah R, Mahen ECS, Nuryantini AY (2017) Synthesis and characterization ofcarbon nanoparticle/PVA/Chitosan for security ink applications. Mater Res Express 4:3. https://doi.org/10.1088/2053-1591/aa6075

Ozcan A (2019) Investigation of the effect of para-amino benzoic acid (PABA) added starch-coated chemicals on the printability

properties of paper. J Appl Biomater Funct Mater 17:1–5. https://doi.org/10.1177/2280800018816012
Pati C, Raza R, Ghosh K (2020) Adenine-linked naphthalimide: a case of selective colorimetric as well as fluorometric sensing of F− and anion-activated moisture detection in organic solvents and CO2-sensing. Spectrochim Acta A Mol Biomol Spectrosc 229:117910. https://doi.org/10.1016/j.saa.2019.117910
Qiu S, Gao Z, Yan F, Yuan H, Wang J, Tian W (2020) 1,8-Dioxapyrene-based electrofluorochromic supramolecular hyperbranched polymers. Chem Commun 56:383–386. https://doi.org/10.1039/c9cc07919j
Rani K, Sengupta S (2021) Multi-stimuli programmable FRET based RGB absorbing antennae towards ratiometric temperature, pH and multiple metal ion sensing. Chem Sci 12:15533–15542. https://doi.org/10.1039/d1sc05112a
Shen Y, Tran TT, Modha S, Tsutsui H, Mulchandani A (2019) A paper-based chemiresistive biosensor employing single-walled carbon nanotubes for low-cost, point-of-care detection. Biosens Bioelectron 130:367–373. https://doi.org/10.1016/j.bios.2018.09.041
Shi X, Yang X, Gai L, Zhou Z, Lu H (2021) NBN unit functionalized pyrene derivatives with different photophysical and anti-counterfeiting properties. J Photochem Photobiol A Chem 412:113206. https://doi.org/10.1016/j.jphotochem.2021.113206
Sonawane SL, Asha SK (2016) Fluorescent polystyrene microbeads as invisible security ink and optical vapor sensor for 4-nitrotoluene. ACS Appl Mater Interfaces 8:10590–10599. https://doi.org/10.1021/acsami.5b12325
Sönmez S, Arslan S (2021) Investigation of the effects on ink colour of lacquer coating applied to the printed substrate in the electrophotographic printing system. Pol J Chem Technol 23:35–40. https://doi.org/10.2478/pjct-2021-0014
Srinivasan V, Khamrang T, Ponraj C, Saravanan D, Yamini R, Bera S, Asha M (2021) Pyrene based Schiff bases : synthesis, crystal structure, antibacterial and BSA binding studies. J Mol Struct 1225:129153. https://doi.org/10.1016/j.molstruc.2020.129153
Tan L, Mo S, Fang B, Cheng W, Yin M (2018) Dual fluorescence switching of a Rhodamine 6G-naphthalimide conjugate with high contrast in the solid state. J Mater Chem C Mater 6:10270–10275. https://doi.org/10.1039/C8TC03654C
Tipsotnaiyana N, Jarupan L, Noppakundilograt S (2015) Enhancement of flexographic print quality on bleached kraft liner using nano-silica from rice husk. Prog Org Coat 87:232–241. https://doi.org/10.1016/j.porgcoat.2015.06.008
Tobias RH, Everett ET (2019) Lightfastness studies of water-based inkjet inks on coated and uncoated papers. In: International conference on digital printing technologies. pp 509–514
Uzun K (2021) Comparison of charge transport and opto-electronic properties of pyrene and anthracene derivatives for OLED applications. J Mol Model 27(6):174. https://doi.org/10.1007/s00894-021-04793-2
Wakchaure VC, Das T, Babu SS (2019) Boron-conjugated pyrenes as fluorescence-based molecular probes and security markers. ChemPlusChem 84:1253–1256. https://doi.org/10.1002/cplu.201900280
Wang G (2021) A pyrene fluorescent probe for rapid detection of ferric ions. J of Fluoresc 31:713–718. https://doi.org/10.1007/s10895-021-02695-3
Wang X, Wang L, Mao X, Wang Q, Mu Z, An L, Zhang W, Feng X, Redshaw C, Cao C, Qin A, Tang BZ (2021) Pyrene-based aggregation-induced emission luminogens (AIEgens) with less colour migration for anti-counterfeiting applications. J Mater Chem C Mater 9:12828–12838. https://doi.org/10.1039/d1tc03022a
Yang S, Wu D, Gong W, Huang Q, Zhen H, Ling Q, Lin Z (2018) Highly efficient room-temperature phosphorescence and afterglow luminescence from common organic fluorophores in 2D hybrid perovskites. Chem Sci 9:8975–8981. https://doi.org/10.1039/c8sc03563f
Yao B, Lin P, Sun H, Wang S, Luo C, Li Z, Du X, Ding Y, Xu Y, Wan H, Zhu W (2021) Janus oligomers demonstrating full-spectrum visible light reflection and tunable photoluminescence towards dual-mode dynamic anti-counterfeiting. Adv Opt Mater 9(5):2001434. https://doi.org/10.1002/adom.202001434